In vivo time-resolved reflectance spectroscopy of the human forehead

Daniela Comelli, Andrea Bassi, Antonio Pifferi, Paola Taroni, Alessandro Torricelli, Rinaldo Cubeddu, Fabrizio Martelli, and Giovanni Zaccanti

We present an *in vivo* broadband spectroscopic characterization of the human forehead. Absorption and scattering properties are measured on five healthy volunteers at five different interfiber distances, using time-resolved diffuse spectroscopy and interpreting data with a model of the diffusion equation for a homogeneous semi-infinite medium. A wavelength-tunable mode-locked laser and time-correlated single-photon counting detection are employed, enabling fully spectroscopic measurements in the range of 700–1000 nm. The results show a large variation in the absorption and scattering properties of the head depending on the subject, whereas intrasubject variations, assessed at different interfiber distances, appear less relevant, particularly for what concerns the absorption coefficient. The high intersubject variability observed indicates that a unique set of optical properties for modeling the human head cannot be used correctly. To better interpret the results of the analysis of *in vivo* measurements, we performed a set of four-layer model Monte Carlo simulations based on different data sets for the optical properties of the human head, partially derived from the literature. The analysis indicated that, when simulated time-resolved curves are fitted with a homogeneous model for the photon migration, the retrieved absorption and reduced scattering coefficients are much closer to superficial layer values (i.e., scalp and skull) than to deeper layer ones (white and gray matter). In particular, for the shorter interfiber distances, the recovered values can be assumed as a good estimate of the optical properties of the first layer.

OCIS codes: 170.5280, 300.6500, 170.7050, 170.3660.

1. Introduction

In past years there has been an increasing demand for a better knowledge of the optical properties of biological tissues for both diagnostic and therapeutic techniques in biomedicine.[1] In particular, the *in vivo* determination of the optical properties of the human head is of the utmost importance due to the increasing application of near-infrared optics in neuroscience.[2] Human brain mapping by functional near-infrared spectroscopy is perhaps the most challenging and fascinating application in this field, while optical techniques are also promising for detection and therapy of neurodegenerative diseases. In the former case, the goal is typically to detect changes in the absorption properties of the brain or cerebral cortex due to the hemodynamic response following functional activation. This is a relative or dynamic problem that is somehow less influenced by the lack of knowledge in the exact optical properties of the human head.[3] On the other hand, absolute determination of the optical parameters is required for static applications such as hematoma detection or light dosimetry for photodynamic therapy.[4]

Indeed from an optical point of view, the head is a strongly heterogeneous structure. Light passes through the scalp, the skull, and the cerebrospinal fluid (CSF) before reaching the brain, typically a few centimeters below the head's surface. All these compartments would affect light propagation in distinct manners. Since *ex vivo* and *post mortem* estimates of optical properties significantly differ from *in vivo* measurements, it is obvious that to obtain an optical characterization of these structures would require

D. Comelli (daniela.comelli@polimi.it), A. Bassi, A. Pifferi, P. Taroni, A. Torricelli, and R. Cubeddu are with the Centre of Ultrafast and Ultraintense Optical Science, Consiglio Nazionale delle Ricerche, Istituto Nazionale di Fisica della Materia and Instituto di Fotonica e Nanotecnologie, Consiglio Nazionale delle Ricerche, Dipartimento di Fisica, Politecnico di Milano, Piazza Leonardo da Vinci 32, I-20133 Milano, Italy. F. Martelli and G. Zaccanti are with the Dipartimento di Fisica, Università degli Studi di Firenze, Via G. Sansone 1, I-50019 Sesto Fiorentino, Firenze, Italy.

Received 18 July 2006; revised 18 October 2006; accepted 17 November 2006; posted 20 November 2006 (Doc. ID 73129); published 13 March 2007.

0003-6935/07/101717-09$15.00/0

access to an operating room during a neurosurgical procedure. An alternative approach is to noninvasively inject light from the head surface and to collect the diffusely remitted photons in different locations in reflectance geometry. This is the approach that has been effectively pursued in recent years by several researchers thanks to its simplicity both for static[5–7] and dynamic (or functional) measurements.[8–11]

However, the attention is then focused on data interpretation, this being an ill-posed inverse problem.[12] To gain insight into the problem of determining optical properties of the head, Monte Carlo (MC) simulations in layered media have been performed, where the head is typically modeled as a stack of independent layers (scalp, skull, CSF, gray matter, white matter) with different geometric and optical properties.[13–23] In parallel, advanced analytical methods based on a solution of the diffusion equation in a two-layered medium have been reported.[24,25]

It should be noted that the robustness of any noninvasive diagnostic procedure to assess absorption and scattering properties of these layers would greatly benefit from *a priori* information as derived, for instance, from computed tomography or magnetic resonance imaging, as has been performed by Barnett *et al.*[26] However, even if detailed anatomical information is obtained, no analytical model would be available to directly interpret spectroscopy data. Therefore the ideal solution would be to use the 3D finite-element model code.

Here we approached the complex study of light propagation in head tissues from an experimental point of view by performing time-resolved multiwavelength, multidistance reflectance measurements on the forehead of adult volunteers. For data analysis, since anatomical information on volunteers's heads were not available, we chose to interpret the measured time-resolved curves using a homogeneous model for photon migration. This simple kind of analysis, even though approximated, is aimed at investigating major spectral variations among different subjects and interfiber distances. We decided not to consider the application of a bilayer model. In fact, this approach, even if possible, leads to a fitting procedure much more unstable and of difficult comprehension with respect to a homogeneous fit, since both optical properties and thickness of the two layers are unknown, which results in a fitting algorithm on six parameters.

As a second step, to better interpret the analysis of our *in vivo* measurements, we performed a set of MC simulations, where the human head was modeled as a four-layer structure characterized by optical properties partially derived from the literature. The simulated time-resolved curves were interpreted in the same way as *in vivo* measurements, using a homogeneous model for photon migration. In this way, we aimed at better comprehending the information carried out by a homogeneous analysis performed on a heterogeneous structure as the human head.

2. Materials and Methods

A. System Setup

The automated system for time-resolved spectroscopy (TRS) measurements has been described in previous publications.[5,27] The system allows fully spectroscopic measurements in the range of 700–1000 nm, exploiting an actively mode-locked picosecond Ti:sapphire laser. A 1 mm plastic–glass fiber (AFS1000, Fiberguide, New Jersey) delivered light into the tissue, while diffusely reflected photons were collected by a 4 mm diameter fiber bundle (Fiberguide, New Jersey). The power at the distal end of the illumination fiber was always limited to less than 10 mW for safety. For detection, we used a double-microchannel-plate photomultiplier tube (R1564U with S1 photocathode, Hamamatsu Photonics K.K., Japan) and a PC card for time-correlated single-photon counting (SPC-130, Becker and Hickl GmbH, Germany). A small fraction of the incident beam was coupled to a 1 mm fiber and fed directly to the photomultiplier tube for on-line recording of the instrument response function (IRF). Overall, the FWHM of the IRF was less than 180 ps at any wavelength.

To allow measurements to be carried out *in vivo*, the system is fully automated. A PC controlled the laser tuning and power, and optimized the IRF by automatically adjusting the Lyot filters and the cavity length of the Ti:sapphire laser. The overall measurement time for a full spectrum at a certain interfiber distance was ~10 min. To handle the large dynamic range these measurements present, a variable neutral density filter was mounted on a stepper motor in the detection line in order to adjust the intensity on the detector. The total number of collected photons per second was used as input in a feedback loop, and we aimed at having a signal of approximately 10^6 counts in 4 s acquisition time per each wavelength.

B. Phantom Measurements

A first series of TRS measurements was performed on a homogeneous cylindrical solid phantom (4.5 cm height, 10.5 cm diameter) made of an epoxy resin, with titanium dioxide (TiO_2) powder as the scatterer and black toner as the absorber.[28] Spectroscopy information was obtained by acquiring time-resolved curves every 5 nm from 700 to 1000 nm. The injection and collection fibers were both placed on the top base of the cylinder and reflectance measurements were collected at five different interfiber distances (from 2 up to 6 cm).

C. Protocol for *In Vivo* Measurements

Five healthy volunteers were enrolled for the measurements after informed consent. No particular preselection of the volunteers was made. The five subjects were three males (25, 37, and 40 years old) and two females (31 and 42 years old). Spectroscopy measurements from 700 to 1000 nm were performed in reflectance mode at the five different interfiber distances. The in-

Table 1. Thickness, μ_a and μ_s' Values at $\lambda = 800$ nm, of the Four-Layer Model of the Human Forehead used for MC Simulations

Layers	Thickness	μ_a (cm^{-1})	Data Set 1 (Ref. 14) μ_s' (cm^{-1})	Data Set 2 (Ref. 16) μ_s' (cm^{-1})	Data Set 3 (Ref. 17) μ_s' (cm^{-1})	Data Set 4 μ_s' (cm^{-1})
Scalp + skull	10 mm	0.15	16.0	9.0	9.5	8.0
CSF	2 mm	0.04	2.5	2.5	2.5	8.0
Gray matter	4 mm	0.19	22	7	8.0	8.0
White matter	∞	0.13	91	40	11.0	8.0

jection and collection fibers were put on the left part of the forehead, with the injection fiber placed toward the temporal region. The collection bundle was set 1 cm on the left of the central sulcus, to avoid interferences caused by the sinovial cavity.

D. Data Analysis

The reduced scattering and absorption spectra were constructed by plotting, versus wavelength, the values of μ_s' and μ_a, as obtained from fitting the experimental data to an analytical solution of the diffusion approximation of the transport equation for a homogeneous semi-infinite medium.[29] We used the extrapolated boundary condition[30] and assumed that the diffusion coefficient D was independent of the absorption properties of the medium [i.e., $D = 1/(3\mu_s')$].[31] The refractive index was assumed equal to 1.56 in the case of the epoxy resin phantom and equal to 1.40 in the case of head tissues.

As shown in detail in Cubeddu *et al.*,[32] the theoretical time-dispersion curve was convolved with the IRF and normalized to the area of the experimental curve. The fitting range included all the points with a number of counts higher than 80% of the peak value on the rising edge of the curve and 1% on the tail. The best fit was reached with a Levenberg–Marquardt algorithm by varying both μ_s' and μ_a to minimize the error norm χ^2.

A brief consideration on the fitting procedure is given here. As previously shown, the use of a free time shift can improve the estimation of the optical properties, although it increases the dispersion of the retrieved values and the instability of the fitting procedure.[32] Thus in order to minimize the differences in the optical properties estimated at the different detection distances and further reduce the coupling between absorption and scattering coefficients, we decided to introduce the same fixed time shift for all wavelengths and interfiber distance measurement analysis. The recovered value of 98 ps for the temporal shift can be possibly attributed to the mode dispersion of the collection fiber as already observed elsewhere.[33]

E. Monte Carlo Model

A MC code based on a four-layer semi-infinite slab model was employed. Details on the MC code can be found elsewhere.[34] The four layers simulate the scalp–skull matter, the CSF layer, the gray matter, and the white matter. The optical properties of the layers (at $\lambda = 800$ nm), were chosen according to four different data sets, partially derived from the literature. In particular, since the models of the optical properties of the human head already discussed in the literature fairly agree concerning absorption properties, whereas they show a much higher discrepancy in the scattering values, we decided to select four possible data sets characterized by the same absorption coefficient values and different scattering properties. Reduced scattering coefficients were selected from Refs. 14, 16, and 17 for the first, second, and third data set, respectively. For the last data set, a uniformly scattering tissue was considered. The

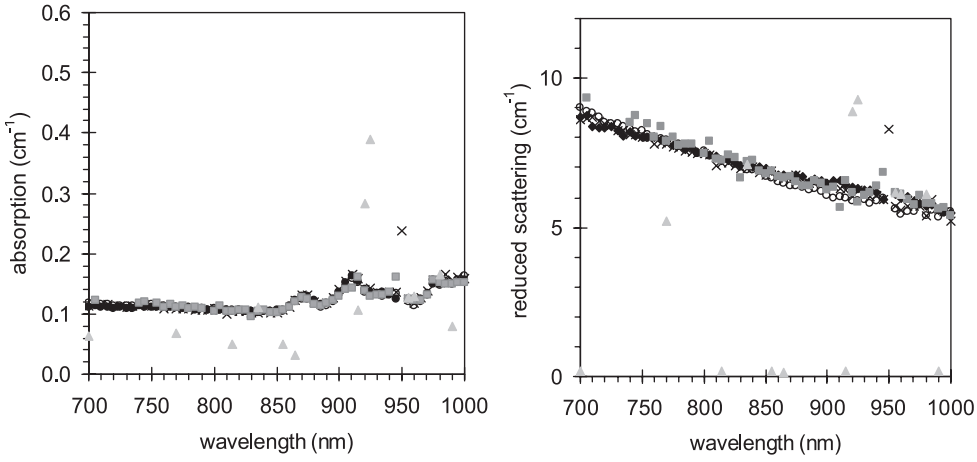

Fig. 1. Absorption spectra (left panel) and reduced scattering spectra (right panel) of a solid phantom made of epoxy resin, titanium oxide powder, and black toner, measured in the reflectance mode at five different interfiber distances (from 2 up to 6 cm).

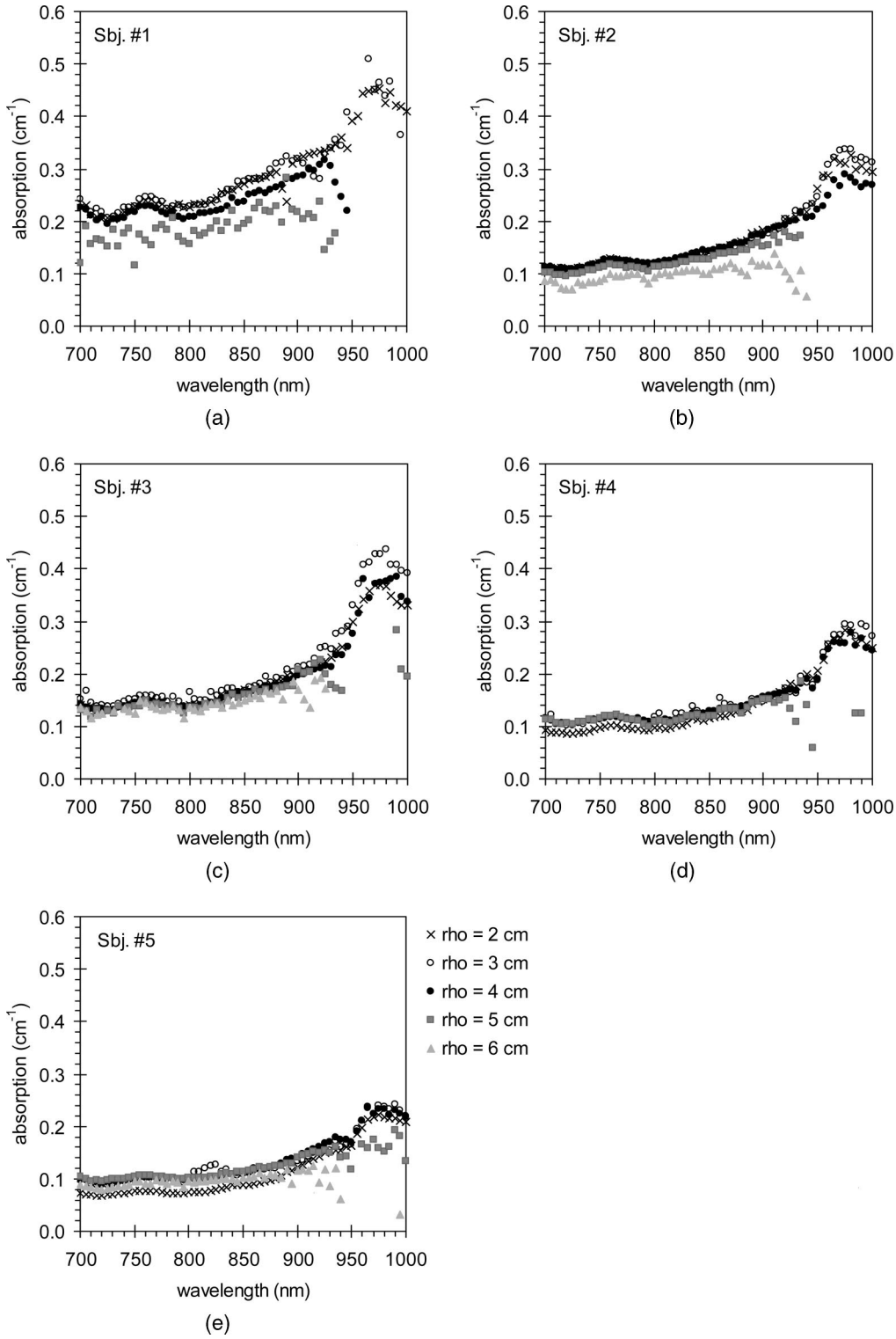

Fig. 2. (a)–(e) Absorption spectra of the forehead of the five volunteers in reflectance mode at five different interfiber distances.

chosen optical coefficients are summarized in Table 1, together with the thickness chosen for each layer. Single-wavelength time-resolved simulated curves at six different interfiber distances (from 1 up to 6 cm) were then fitted with the same procedure as used for *in vivo* time-resolved data on the basis of a homogeneous model for the human head.

3. Measurements

A. Phantom Measurements

Figure 1 shows the absorption coefficient and the reduced scattering coefficient spectra of the phantom measured at the five different interfiber distances. As expected, in the presence of a homogeneous sample

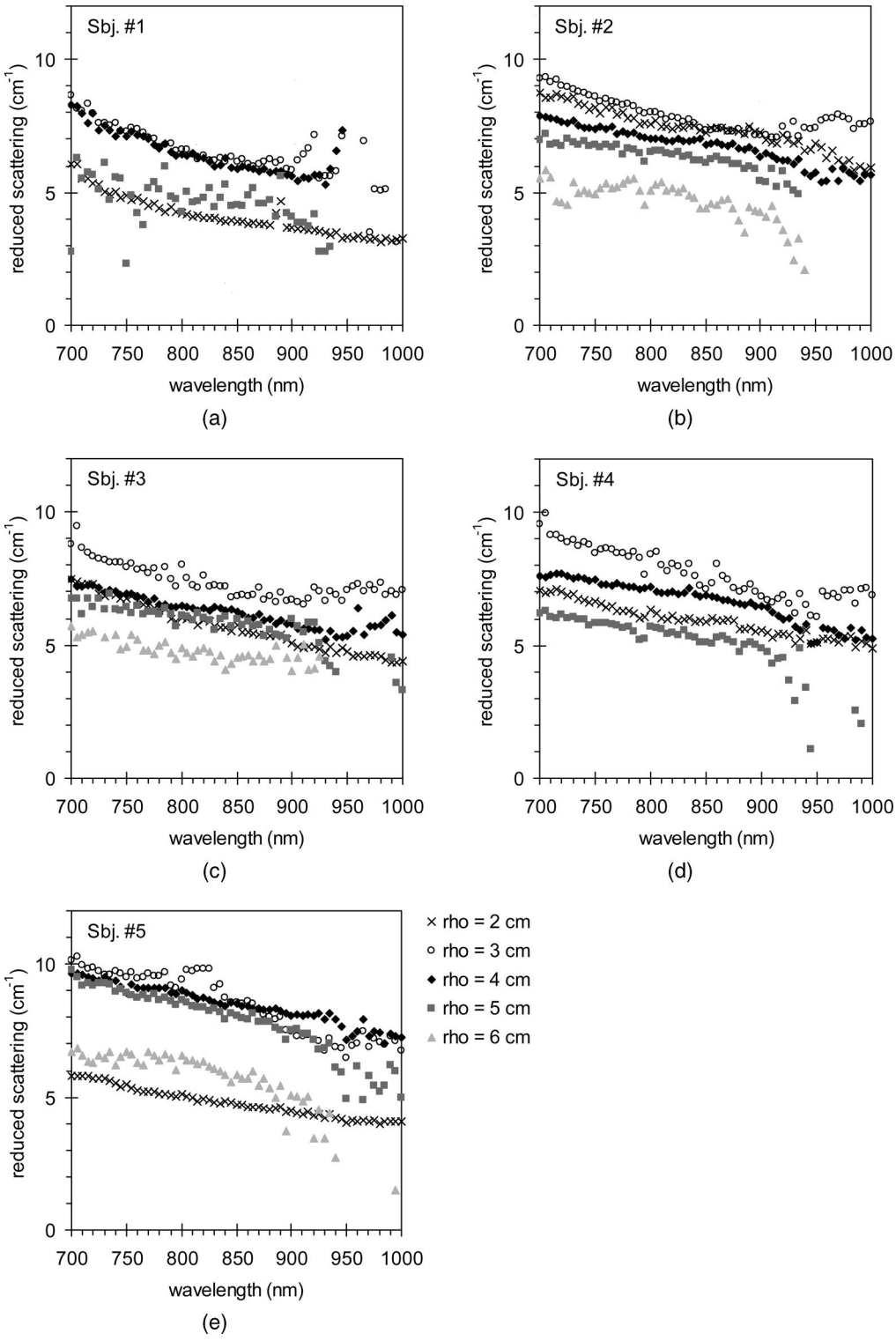

Fig. 3. (a)–(e) Reduced scattering spectra of the forehead of the five volunteers in reflectance mode at five different interfiber distances.

there is no detectable variation in the measured optical properties by varying the collection distance; consequently, the recovered spectra appear almost identical at all the distances. Focusing deeply on the shape of the spectra, as shown elsewhere,[28] the absorption coefficient exhibits a rather flat plateau below 850 nm, owing mainly to the toner absorption, and higher peaks beyond 850 nm, ascribed to the resin contribution. With respect to the scattering coefficient, as expected, decreasing values of μ_s' are reconstructed upon increasing wavelength. Finally, it can be observed that the measurement at the largest

collection distance was poorly analyzed since a few number of photons reached the detector.

B. *In Vivo* Measurements

In vivo absorption and reduced scattering spectra are shown in Figs. 2 and 3, respectively. For subject 1 reliable optical coefficients could not be recovered at any wavelength at $\rho = 6$ cm, as a consequence of the high absorption that characterizes the forehead of this volunteer. Further, for subject 4 the measurement at $\rho = 6$ cm was not performed at all due to a technical failure. For the remaining subjects the spectra at the largest interfiber distance, even though noisy, could be analyzed apart from the region of the water peak absorption near 970 nm. This consideration briefly indicates that the attenuation of light in the human head, due to both absorbers and scatterers, is smaller than that of a homogeneous diffusing media as the solid phantom considered.

Absorption spectra for all the subjects at the different interfiber distances are shown in Figs. 2(a)–2(e). Similar spectral shapes are generally retrieved among subjects with the evidence of the main peak absorbers, as deoxy-hemoglobin at 760 nm and water at 970 nm. However, the absorption coefficient shows a large variation from subject to subject. In contrast, absorption spectra show similar features at all interfiber distances. For example, focusing on the spectra of subject 3, the hemoglobin peak, centered near 760 nm, is clearly visible with a similar absorption value at all the interfiber distances; at longer wavelengths the dominant absorption feature is the water peak at ~970 nm, with a decreasing absorption coefficient measured at distances longer than 3 cm. Further, the lipid peak at 930 nm is slightly visible only at the longest interfiber distances. This last observation could correlate with a significant lipid content present in deeper tissues.

To evaluate the percentage composition of the head tissues of different volunteers, the absorption spectra were best fitted with a linear combination of the spectra of the main tissue constituents but satisfactory results could not be achieved. As typically performed,[5] lipid, water, and the two forms of hemoglobin were taken into account as the main tissue absorbers. In this case study, we further considered the presence of collagen, whose absorption spectrum has been recently measured by us,[35] as a possible absorber in the bone tissue of the skull. Nevertheless, in some of the cases, the fitting procedure could not converge to a stable solution, since it was heavily dependent on the initial conditions. It should be noted that in this case study we recorded time-resolved spectra only in the near-infrared band from 700 to 1000 nm, whereas the red spectral band from 600 to 695 nm could not be explored due to a malfunctioning of our tunable red laser source. The red spectral band, where the two forms of hemoglobin show high absorption values, is particularly important in tissue component analysis and, possibly, its absence gives less stability to the fitting procedure. Further, another cause could be found in the heterogeneous structure of the head.

For what concerns the reduced scattering coefficient, the retrieved spectra for all the subjects are shown in Figs. 3(a) through 3(e). Scattering spectra show decreasing values of μ_s' with increasing wavelength. Significant variations are observed among subjects. Further, conversely from the absorption spectra, the scattering spectra showed detectable differences at the five interfiber distances both for what concerns the amplitude and the slope of the spectra. In particular, as a general trend, the highest-scattering values are retrieved at an interfiber distance of 3 cm, while lower-scattering values are measured as interfiber distance increases.

4. Discussion

A. Discussion on *In Vivo* Measurements

In vivo absorption and reduced scattering spectra of the human forehead revealed marked differences among volunteers. To emphasize this variability, in Fig. 4 the spectra of the five volunteers measured at

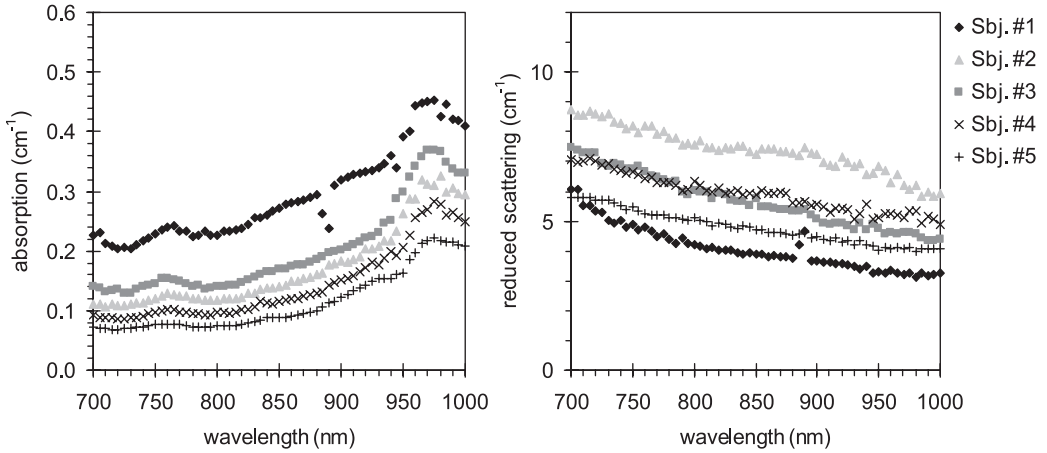

Fig. 4. Absorption spectra (left panel) and reduced scattering spectra (right panel) of the forehead of the five volunteers acquired in reflectance mode at the shortest interfiber distance ($\rho = 2$ cm).

Table 2. Hemoglobin Concentrations, Total Hemoglobin Content, and Hemoglobin Oxygen Saturation[a]

Volunteer	Hb (μM)	HbO_2 (μM)	THC (μM)	Y (%)
1	43.4	81.2	124.5	65.2
2	21.3	42.4	63.7	66.5
3	27.1	49.3	76.4	64.5
4	16.9	35.1	52.0	67.6
5	14.0	26.1	40.1	65.1

[a]Deoxy-hemoglobin (Hb) concentration, oxy-hemoglobin (HbO_2) concentration, total hemoglobin content (THC), and hemoglobin oxygen saturation (Y) of the superficial head tissues estimated for the five subjects considering the absorption spectra retrieved at the shortest interfiber distance ($\rho = 2$ cm).

the shortest interfiber distance ($\rho = 2$ cm) are presented.

Absorption spectra show a net variation in the retrieved coefficient values: differences up to a maximum factor of 3 can be found in the absorption values of different subjects at the same wavelength. This high intersubject variability in the absorption spectra can be ascribed to a different skull thickness or to the presence of tissues characterized by a different blood perfusion or, more probably, to both these two phenomena.

At the moment, we cannot validate the first hypothesis since we have no quantitative information on the anatomy of the head of the five volunteers. For what concerns the second hypothesis, we considered the differences in hemoglobin concentrations between subjects taking into account the *in vivo* absorption spectra plotted in Fig. 4. The analysis was performed considering the two forms of hemoglobin as the only tissue absorbers and considering absorption spectra in the range of 700–850 nm, where the absorption of oxy- and deoxy-hemoglobin predominate with respect to other tissue absorbers; the results are summarized in Table 2 in terms of hemoglobin concentrations, total hemoglobin content, and hemoglobin oxygen saturation.[5] The analysis indicates that absorption spectral variations can be explained by marked differences in the total hemoglobin content, which shows a variation from 40 to 125 μM from subject to subject. Similarly, the scattering spectra measured on the five volunteers at the shortest interfiber distance revealed a detectable variability among subjects.

We believe that these high differences in both the absorption and the scattering properties of the head of volunteers is an important indication that should be taken into account when modeling light propagation in the human head; in particular, it should be emphasized that a unique data set for the optical properties of the human head cannot be reliable.

B. Comparison with Monte Carlo Simulations

To interpret the results of the homogeneous analysis performed on *in vivo* measurements, we applied the same homogeneous analysis on MC time-resolved simulated curves. Table 3 shows the absorption and scattering coefficient obtained by fitting the four-layer MC simulations with the homogeneous model.

It appears evident that the retrieved absorption coefficient values at all six interfiber distances are very close to one other, with a maximum relative variation between values from the same data set of 6%. It is worthwhile to observe that experimental data, analyzed with the same homogeneous model, show similar changes with different interfiber distances: taking into account the absorption coefficients obtained for the same subject and focusing on the shorter distances (from 2 up to 4 cm), where the measurements are less critical in terms of signal-to-noise ratio, it is possible to observe a maximum relative variation of 10% at 800 nm.

MC simulations further indicate that the retrieved absorption coefficient is very close to the value of the superficial layer (i.e., scalp and skull), as if photons detected even at the larger interfiber distances had traveled much more in the first layer than in deeper ones; a possible explanation can be found in the low-scattering properties of the CSF, which acts as an optical guide for photons. This result is particularly valuable when extended to *in vivo* measurements: the recovered values for shorter interfiber distances can in fact be assumed as a good estimate of the absorption properties of the scalp–skull layer.

For what concerns the reduced scattering coefficient, the values obtained when fitting simulated MC data appear again closer to the value of the first layer with respect to the value of the underlying structures. Nevertheless, in this case the extraction of informa-

Table 3. μ_a and μ_s' Values Retrieved by Fitting the Four-Layer MC Simulations with a Homogeneous Model for the Human Head

Interfiber Distance ρ (cm)	Data Set 1		Data Set 2		Data Set 3		Data Set 4	
	μ_a (cm^{-1})	μ_s' (cm^{-1})	μ_a (cm^{-1})	μ_s' (cm^{-1})	μ_a (cm^{-1})	μ_s' (cm^{-1})	μ_a (cm^{-1})	μ_s' (cm^{-1})
1	0.15	16.0	0.14	8.12	0.15	8.93	0.14	6.40
2	0.14	16.3	0.13	8.83	0.14	9.42	0.14	7.57
3	0.15	17.1	0.14	9.71	0.14	9.79	0.14	8.13
4	0.15	14.7	0.15	9.06	0.14	9.02	0.14	8.04
5	0.14	12.4	0.15	8.15	0.14	8.35	0.14	8.02
6	0.14	11.2	0.15	7.69	0.14	7.57	0.14	8.15

tion is less straightforward, since there is a much higher variation of the retrieved scattering values with interfiber distance, both considering analysis on *in vivo* measurements and MC simulated data.

However, it is valuable to observe that the comparison between simulated and *in vivo* analysis shows an interesting common feature. Considering the results at different interfiber distances both analyses indicate that, as a general trend, the scattering value, after a first small increase that reaches its maximum at $\rho = 3$ cm, decreases at longer interfiber distances. The decrease can again be due to the presence of the low-scattering CSF, whose effect becomes more relevant at longer interfiber distances. For MC simulations, this effect is particularly marked for the first data set, which is characterized by a higher-scattering value of the scalp–skull layer. Thus even for the case of scattering, we can assume that the values obtained at shorter interfiber distances are the least influenced by underlying layers and, consequently, can be considered as an initial estimation of the scattering properties of the superficial layer of the head.

5. Conclusion

In conclusion, we have performed an *in vivo* spectral characterization of the human forehead with time-resolved reflectance measurements at multiple interfiber distances. Although, the data were interpreted using a homogeneous model of photon migration, the recovered spectra yield useful information on the optical properties of the superficial layers, as also confirmed by Monte Carlo simulations. Work is in progress both to get anatomical information for the volunteers' heads and to apply a more refined heterogeneous model to *in vivo* measurements in order to investigate deeper structures. Further, the collection of data in the red spectral band could be beneficial for the quantification of main tissue absorbers.

This work was partially supported by Ministero Italiano dell' Università e della Ricerca under project PRIN2005 (contract 2005025333).

References

1. For latest results see Biomedical Topical Meetings on CD-ROM (Optical Society of America, 2006).
2. D. A. Boas and R. D. Frostig, "Optics in neuroscience," J. Biomed. Opt. **10,** 011001 (2005).
3. A. P. Gibson, J. C. Hebden, and S. R. Arridge, "Recent advances in diffuse optical imaging," Phys. Med. Biol. **50,** R1–R43 (2005).
4. H. Kostron, A. Obwegeser, and R. Jakober, "Photodynamic therapy in neurosurgery: a review," J. Photochem. Photobiol. B **36,** 157–168 (1996).
5. A. Torricelli, A. Pifferi, P. Taroni, E. Giambattistelli, and R. Cubeddu "*In vivo* optical characterization of human tissues from 610 to 1010 nm by time-resolved reflectance spectroscopy," Phys. Med. Biol. **46,** 2227–2237 (2001).
6. M. Firbank, C. E. Elwell, C. E. Cooper, and D. T. Delpy, "Experimental and theoretical comparison of NIR spectroscopy measurements of cerebral hemoglobin changes," J. Appl. Physiol. **85,** 1915–1921 (1998).
7. J. Choi, M. Wolf, V. Toronov, U. Wolf, C. Polzonetti, D. Hueber, L. P. Safonova, R. Gupta, A. Michalos, W. Mantulin, and E. Gratton, "Noninvasive determination of the optical properties of adult brain: near-infrared spectroscopy approach," J. Biomed. Opt. **9,** 221–229 (2004).
8. D. Contini, A. Torricelli, A. Pifferi, L. Spinelli, F. Paglia, and R. Cubeddu, "Multi-channel time-resolved system for functional near infrared spectroscopy," Opt. Express **14,** 5418–5432 (2006).
9. J. Selb, M. A. Franceschini, A. G. Sorensen, and D. A. Boas, "Improved sensitivity to cerebral hemodynamics during brain activation with a time-gated optical system: analytical model and experimental validation," J. Biomed. Opt. **10,** 011013 (2005).
10. G. Strangman, D. A. Boas, and J. P. Sutton, "Non-invasive neuroimaging using near-infrared light," Biol. Psychiatry **52,** 679–693 (2002).
11. A. Villringer and B. Chance, "Noninvasive optical spectroscopy and imaging of human brain function," Trends Neurosci. **20,** 435–442 (1997).
12. S. R. Arridge, "Optical tomography in medical imaging," Inverse Probl. **15,** R41–R93 (1999).
13. Y. Fukui, Y. Ajichi, and E. Okada, "Monte Carlo prediction of near-infrared light propagation in realistic adult and neonatal head models," Appl. Opt. **42,** 2881–2887 (2003).
14. E. Okada and D. T. Delpy, "Near-infrared light propagation in an adult head model. I. Modeling of low-level scattering in the cerebrospinal fluid layer," Appl. Opt. **42,** 2906–2914 (2003).
15. E. Okada and D. T. Delpy, "Near-infrared light propagation in an adult head model. II. Effect of superficial tissue thickness on the sensitivity of the near-infrared spectroscopy signal," Appl. Opt. **42,** 2915–2922 (2003).
16. A. N. Yaroslavsky, P. C. Schulze, I. V. Yaroslavsky, R. Schober, F. Ulrich, and H. J. Schwarzmaier, "Optical properties of selected native and coagulated human brain tissues in vitro in the visible and near infrared spectral range," Phys. Med. Biol. **47,** 2059–2073 (2002).
17. F. Bevilacqua, D. Piguet, P. Marquet, J. D. Gross, B. J. Tromberg, and C. Depeursinge, "*In vivo* local determination of tissue optical properties: applications to human brain," Appl. Opt. **38,** 4939–4950 (1999).
18. M. Firbank, S. R. Arridge, M. Schweiger, and D. T. Delpy, "An investigation of light transport through scattering bodies with non-scattering regions," Phys. Med. Biol. **41,** 767–783 (1996).
19. A. H. Hielscher, R. E. Alcouffe, and R. L. Barbour, "Comparison of finite-difference transport and diffusion calculations for photon migration in homogeneous and heterogeneous tissues," Phys. Med. Biol. **43,** 1285–1302 (1998).
20. H. Dehghani, S. R. Arridge, M. Schweiger, and D. T. Delpy, "Optical tomography in the presence of void regions," J. Opt. Soc. Am. A **17,** 1659–1670 (2000).
21. E. Okada and D. T. Delpy, "Effect of discrete scatterers in CSF layer on optical path length in the brain," in *Diffuse Spectroscopy and Optical Coherence Tomography: Imaging and Functional Assessment,* S. Andersson-Engels and J. G. Fujimoto, eds., Proc. SPIE **4160,** 196–203 (2000).
22. A. Custo, W. M. Wells, A. H. Barnett, E. M. C. Hillman, and D. A. Boas, "Effective scattering coefficient of the cerebral spinal fluid in adult head models for diffuse optical imaging," Appl. Opt. **45,** 4747–4755 (2006).
23. A. H. Hielscher, H. Liu, B. Chance, F. K. Tittel, and S. L. Jacques, "Time-resolved photon emission from layered turbid media," Appl. Opt. **35,** 719–728 (1996).
24. F. Martelli, A. Sassaroli, G. Del Bianco, S. Yamada, and G. Zaccanti, "Solution of the time-dependent diffusion equation for layered diffusive media by the eigenfunction method," Phys. Rev. E **67,** 056623 (2003).
25. A. Kienle, M. S. Patterson, N. Dognitz, R. Bays, G. Wagnieres, and H. van den Bergh, "Noninvasive determination of the

optical properties of two-layered turbid media" Appl. Opt. **37,** 779–791 (1998).
26. A. H. Barnett, J. P. Culver, A. G. Sorensen, A. Dale, and D. A. Boas "Robust inference of baseline optical properties of the human head with three-dimensional segmentation from magnetic resonance imaging," Appl. Opt. **42,** 3095–3108 (2003).
27. R. Cubeddu, A. Pifferi, P. Taroni, A. Torricelli, and G. Valentini, "Time-resolved reflectance spectroscopy in tissues," in *Laser-Tissue Interaction X: Photochemical, Photothermal, and Photomechanical,* S. L. Jacques, G. J. Muller, A. Roggan, and D. H. Sliney, eds., Proc. SPIE **3601,** 486–490 (1999).
28. A. Pifferi, A. Torricelli, A. Bassi, P. Taroni, R. Cubeddu, H. Wabnitz, D. Grosenick, M. Möller, R. Macdonald, J. Swartling, T. Svensson, S. Andersson-Engels, R. L. P. van Veen, H. J. C. M. Sterenborg, J. M. Tualle, H. L. Nghiem, S. Avrillier, M. Whelan, and H. Stamm, "Performance assessment of photon migration instruments: the MEDPHOT protocol," Appl. Opt. **44,** 2104–2114 (2005).
29. M. S. Patterson, B. Chance, and B. C. Wilson, "Time-resolved reflectance and transmittance for the noninvasive measurement of tissue optical properties," Appl. Opt. **28,** 2331–2336 (1989).
30. R. C. Haskell, L. O. Svasaand, T. T. Tsay, T. C. Feng, M. S. McAdams, and B. J. Tromberg, "Boundary conditions for the diffusion equation in radiative transfer," J. Opt. Soc. Am. A **11,** 2727–2741 (1994).
31. K. Furutsu and Y. Yamada, "Diffusion approximation for a dissipative random medium and the applications," Phys. Rev. E **50,** 3634–3640 (1994).
32. R. Cubeddu, A. Pifferi, P. Taroni, A. Torricelli, and G. Valentini, "Experimental test of theoretical models for time-resolved reflectance," Med. Phys. **23,** 1625–1633 (1996).
33. A. Liebert, H. Wabnitz, D. Grosenick, and R. Macdonald, "Fiber dispersion in time domain measurements compromising the accuracy of determination of optical properties of strongly scattering media," J. Biomed. Opt. **8,** 512–516 (2003).
34. F. Martelli, A. Sassaroli, Y. Yamada, and G. Zaccanti, "Analytical approximate solutions of the time-domain diffusion equation in layered slabs," J. Opt. Soc. Am. A **19,** 71–80 (2002).
35. P. Taroni, D. Comelli, A. Pifferi, A. Torricelli, and R. Cubeddu, "Absorption properties of breast: the contribution of collagen," presented at the Biomedical Optics Topical Meeting, Fort Lauderdale, Fla. (19–22 March 2006).